Heme oxygenase-1 contributes to pathology associated with thrombin-induced striatal and cortical injury in organotypic slice culture

Masatoshi Ohnishi[1], Hiroshi Katsuki[2], Kazuhiro Unemura[3] Yasuhiko Izumi[3], Toshiaki Kume[3], Yuki Takada-Takatori[4], and Akinori Akaike[3]

[1]Department of Pharmacotherapeutics, Faculty of Pharmacy and Pharmaceutical Science, Fukuyama University, Gakuencho-1, Fukuyama, Hiroshima 729-0292, Japan.

[2]Department of Chemico-Pharmacological Sciences, Graduate School of Pharmaceutical Sciences, Kumamoto University, 5-1 Oe-honmachi, Kumamoto 862-0973, Japan.

[3]Department of Pharmacology, Graduate School of Pharmaceutical Sciences, Kyoto University, 46-29 Yoshida-shimoadachi-cho, Sakyo-ku, Kyoto 606-8501, Japan.

[4]Department of Pharmacology, Faculty of Pharmaceutical Sciences, Doshisha Women's College, Kodo, Kyotanabe, Kyoto 610-0395, Japan.

Total pages: 31 (including figures)

Address correspondence to Akinori Akaike, Ph.D.

Department of Pharmacology,

Graduate School of Pharmaceutical Sciences, Kyoto University

46-29 Yoshida-shimoadachi-cho, Sakyo-ku, Kyoto 606-8501, Japan.

Phone: +81-75-753-4550 FAX: +81-75-753-4579

E-mail: aakaike@pharm.kyoto-u.ac.jp

ABSTRACT

The blood coagulation factor thrombin that leaks from ruptured vessels initiates brain tissue damage after intracerebral hemorrhage. We have recently shown that mitogen-activated protein kinases (MAPKs) activated by thrombin exacerbate hemorrhagic brain injury via supporting survival of neuropathic microglia. Here, we investigated whether induction of heme oxygenase (HO)-1 is involved in these events. Zinc protoporphyrin IX (ZnPP IX), a HO-1 inhibitor, attenuated thrombin-induced injury of cortical cells in a concentration-dependent manner (0.3-3 μM) and tended to inhibit shrinkage of the striatal tissue at 0.3 μM. HO-1 expression was induced by thrombin in microglia and astrocytes in both the cortex and the striatum. The increase of HO-1 protein was suppressed by a p38 MAPK inhibitor SB203580, and early activation of p38 MAPK after thrombin treatment was observed in neurons and microglia in the striatum. Notably, concomitant application of a low concentration (0.3 μM) of ZnPP IX with thrombin induced apoptotic cell death in striatal microglia and significantly decreased the number of activated microglia in the striatal region. On the other hand, a carbon monoxide releaser reversed the protective effect of ZnPP IX on thrombin-induced injury of cortical cells. Overall, these results suggest that p38 MAPK-dependent induction of HO-1 supports survival of striatal microglia during thrombin insults. Thrombin-induced cortical injury may be also regulated by the expression of HO-1 and the resultant production of heme degradation products such as carbon monoxide.

Section : 8. Disease-Related Neuroscience

Keywords: HO-1; p38 MAPK; microglia; hemorrhagic stroke; apoptosis; striatum

ABBREVIATIONS

ERK: extracellular signal-regulated kinase

HO: heme oxygenase

JNK: c-Jun *N*-terminal kinase

MAPK: mitogen-activated protein kinase

Nrf2: nuclear respiratory factor

PAR: protease-activated receptor

RuCO: tricarbonyldichlororuthenium (II) dimmer

ZnPP IX: zinc (II) protoporphyrin IX

INTRODUCTION

Blood intrinsic factors leak into brain parenchyma during hemorrhagic stroke (Park et al., 2005; Belayev et al., 2005). Among these factors, thrombin plays an important role in the pathogenesis of intracerebral hemorrhage, while it is well known as a blood coagulation factor (Kitaoka et al., 2002; Xi et al., 2006). Serine protease activity of thrombin cleaves proteinase-activated receptors in neurons and glia, resulting in neuronal injury and glial overactivation (Flynn and Buret, 2004; Striggow et al., 2001; Noorbakhsh et al., 2003). Stimulation of proteinase-activated receptors drives a variety of intracellular signaling, including mitogen-activated protein kinase (MAPK) pathways (Marinissen et al., 2003; Suo et al., 2003; Wang et al., 2002). Our previous studies have shown that inhibition of extracellular signal-regulated kinase (ERK), p38 MAPK and c-Jun *N*-terminal kinase (JNK) attenuates thrombin-induced injury of striatal tissue in both *in vitro* and *in vivo* models (Fujimoto et al., 2006, 2007). Interestingly, these MAPK inhibitors induce apoptotic cell death in activated microglia, which may contribute to the neuroprotective effect of these drugs in collagenase-induced intracerebral hemorrhage model *in vivo* and in thrombin-treated corticostriatal slice cultures (Ohnishi et al., 2007; Ohnishi et al., 2010). These effects of MAPK inhibitors suggest that MAPKs are required to maintain survival of activated microglia in hemorrhagic brain. However, detailed mechanisms of MAPK-mediated maintenance of microglial survival remain to be explored.

Heme oxygenase (HO)-1 is an inducible isoform of heme-degrading enzyme whose expression is regulated by MAP kinases as well as by nuclear respiratory factor 2 (Nrf2; Ryter et al., 2006). In hemorrhagic brain of mice, HO-1 expression is mainly observed in microglia/macrophages and vascular endothelial cells around the hematoma region. Deletion of HO-1 gene results in diminution of hemorrhage-induced brain tissue injury (Wang and Doré, 2007). Notably, HO-1 deletion is also associated with a decreased number of

activated microglia/macrophages after intracerebral hemorrhage (Wang and Doré, 2007), suggesting that HO-1 supports survival of activated microglia. Another line of evidence suggesting the role of HO-1 in microglia is that microglial BV-2 cells expressing HO-1 are resistant to various cytotoxic factors such as staurosporine and nitric oxide (Lee and Suk, 2007).

Accordingly, the present study was aimed to reveal whether HO-1 is involved in MAPK-dependent survival of activated microglia and contributes to pathological events under hemorrhagic conditions. For this purpose, we used thrombin-induced injury model of organotypic corticostriatal slice cultures.

RESULTS

HO-1 inhibitor attenuates thrombin-induced cortical cell injury

As reported previously by us (Fujimoto et al., 2006; Ohnishi et al., 2009; Ohnishi et al., 2010), application of 100 U/ml thrombin to corticostriatal slice cultures for 72 h led to substantial cell death in the cortical region as revealed by an increase in the intensity of propidium iodide fluorescence. In addition, thrombin at 100 U/ml induced prominent shrinkage of the striatal region. First we examined the effect of ZnPP IX, a HO-1 inhibitor, on thrombin-induced injury. Thrombin-induced injury in the cortical region was attenuated by concomitant application of ZnPP IX (0.3–3 μM) for 72 h in a concentration-dependent manner, and the effect reached statistical significance at 1 and 3 μM (Figs. 1A–G). As for the striatal region, ZnPP IX tended to suppress thrombin-induced shrinkage of the striatal tissue at 0.3 μM, although the effect diminished as the concentration of ZnPP IX increased to 1 and 3 μM (Figs. 1A–F, H). ZnPP IX at concentrations lower than 0.3 μM had no significant effect (data not shown).

HO-1 expression is induced in glial cells by thrombin

Next we examined profiles of HO-1 expression in corticostriatal slice cultures. Western blot analysis of whole slice cultures revealed that expression of HO-1 was robustly increased after 12 h of thrombin treatment (Figs. 2A and B). To identify cell types expressing HO-1, double immunofluorescence staining with a neuronal marker (MAP-2), a microglial marker (Iba1) and an astrocyte marker (GFAP) was performed in slices treated with thrombin for 24 h. HO-1 expression was observed in microglia and astrocytes but not in neurons in both cortical and striatal regions (Figs. 2C–K). Double immunofluorescence staining with NeuN also confirmed that HO-1 was not expressed in neurons (data not shown).

p38 MAPK mediates HO-1 expression by thrombin

To investigate the involvement of MAP kinase pathways in thrombin-induced expression of HO-1, we examined the effects of MAPK inhibitors. Inhibitors of MAPK/ERK kinase (PD98059), p38 MAPK (SB203580), or JNK (SP600125) were applied at 100 μM concomitantly with 100 U/ml thrombin for 24 h. As shown in Fig. 3, inhibition of p38 MAPK by SB203580 potently and significantly suppressed thrombin-induced increase in HO-1 expression. In contrast, PD98059 and SP600125 had no significant effect.

In a previous study, we demonstrated that thrombin-induced phosphorylation of p38 MAPK peaked at 1 h in corticostriatal slice cultures (Ohnishi et al., 2010). Accordingly, we examined slice cultures treated with thrombin for 1 h, by double immunofluorescence staining to reveal which cell types were responsible for the increase in p38 MAPK phosphorylation. In the striatal region, the phosphorylated form of p38 MAPK colocalized with immunoreactivity against OX42, a microglial marker, as well as that against NeuN, a neuronal marker. Astrocytes, identified by GFAP immunoreactivity, did not exhibit immunopositive signals against phosphorylated p38 MAPK (Fig. 4). p38 MAPK phosphorylation was not evident in the cortical region.

HO-1 inhibitor induces apoptotic cell death in striatal microglia

Both activation of p38 MAPK and expression of HO-1 were observed in striatal microglia after thrombin treatment (Figs. 2F–H and 4D–F). In addition, SB203580 suppressed thrombin-induced increase of HO-1 expression (Fig. 3). Moreover, we have shown previously that MAPKs including p38 MAPK maintain survival of microglia activated by thrombin (Ohnishi et al., 2007; Ohnishi et al., 2010). These findings are consistent with the idea that p38 MAPK-mediated expression of HO-1 is involved in microglial survival. Therefore, we examined the effect of ZnPP IX on the viability of microglia in

thrombin-treated slice cultures. As reported (Ohnishi et al., 2010), 72-h application of 100 U/ml thrombin robustly increased the number of OX42-positive activated microglia in the striatal region. ZnPP IX at 0.3 μM concomitantly applied with thrombin attenuated the increase of microglia (Figs. 5A–D), although higher concentrations (1 and 3 μM) of this compound were less effective.

We further examined the effect of 0.3 μM ZnPP IX with regard to the ability to induce cell death in microglia by examining nuclear condensation and fragmentation. In this context, we have previously demonstrated that thrombin in the presence, but not in the absence, of MAPK inhibitors induces apoptotic changes in nuclear morphology in microglia (Ohnishi et al., 2010). Here, Hoechst 33342 staining combined with OX42 immunofluorescence histochemistry revealed that concomitant application of 0.3 μM ZnPP IX with 100 U/ml thrombin for 48 h induced nuclear condensation and fragmentation in a significant population of microglia in the striatal region (Figs. 5E–I).

Possible involvement of carbon monoxide in HO-1-mediated cortical cell injury

The above results suggest that HO-1 maintains survival of activated microglia to accelerate thrombin-induced striatal cell injury. However, this scenario does not apply to the case with the cortex because thrombin induces cortical cell injury in a microglia-independent manner (Fujimoto et al., 2006). To gain insights into the mechanisms of the effect of ZnPP IX on cortical cell injury (Fig. 1), we examined possible involvement of heme catabolites produced by HO-1 enzymatic activity in thrombin-induced cell death. HO-1 catabolizes heme into carbon monoxide, biliverdin, and free iron. Biliverdin is subsequently metabolized by biliverdin reductase to bilirubin (Maines, 1988), which, in general, shows cytoprotective activity (Doré et al., 1999; Yamamoto et al., 2010). Indeed, application of bilirubin (1–100 μM) to slice cultures did not induce cell death (data not shown). Then, we

tested the effects of a carbon monoxide releaser RuCO, and an iron chelator deferoxamine. The Protective effect of 3 μM ZnPP IX against thrombin-induced cortical cell injury was reversed by RuCO at concentrations of 10 and 30 μM, a concentration range that showed no cytotoxicity by itself (Fig. 6A). In addition, higher concentrations of RuCO alone increased propidium iodide fluorescence in the cortical region in a concentration-dependent manner, and significant cytotoxicity was observed at 300 μM (data not shown). On the other hand, deferoxamine (3–30 μM) partially attenuated thrombin cytotoxicity. The protective effect of deferoxamine reached statistical significance at 10 μM but did not show concentration dependency (Fig. 6B). We could not examine the effect of another iron chelator, phenanthroline, due to the cytotoxicity of its own.

DISCUSSION

The initial aim of the present study was to reveal whether HO-1 was involved in MAPK-dependent microglial survival that may exacerbate hemorrhage-associated brain injury. The results indicated that thrombin application to corticostriatal slice cultures induced HO-1 in striatal microglia in a p38 MAPK-dependent manner, which participated in microglial survival in the striatum. On the other hand, we also found that HO-1 may be involved in cortical cell injury via generation of heme degradation products such as carbon monoxide.

After application of thrombin, HO-1 expression was induced in microglia and astrocytes but not in neurons, both in the cortex and in the striatum. These profiles are reminiscent of the expression pattern in the brain after intracerebral hemorrhage, where microglia/macrophages or endothelial cells around hemorrhage region, but not neurons, show intense HO-1 expression (Wang and Doré, 2007). The major signaling pathway leading to HO-1 induction involves activation of Nrf2 by oxidative stress (Prestera et al., 1995; Alam et al., 1999), but other signaling pathways can be also involved (Ryter et al., 2006). Of members of MAPK family, ERK and p38 MAPK are implicated in HO-1 expression in macrophages (Chen et al., 2002; Lee et al., 2003). In the present study, SB203580 substantially inhibited HO-1 induction, suggesting that p38 MAPK plays a major role in HO-1 expression in thrombin-treated slice cultures. In this context, a recent study demonstrated that methamphetamine-induced HO-1 expression in primary cortical neuron/glia cocultures was dependent on p38 MAPK but not on ERK or JNK (Huang et al., 2009). p38 MAPK may contribute to HO-1 expression by promoting nuclear translocation of Nrf2 (Hwang and Jeong, 2008). We also demonstrated that, in the striatal region, p38 MAPK phosphorylation is induced by thrombin in microglia as well as in neurons. These results are consistent with the idea that p38 MAPK mediates HO-1 induction by thrombin in striatal microglia.

The number of OX42-positive activated microglia increased in response to thrombin. This is consistent with our previous study (Ohnishi et al., 2010) and also with a study by another group demonstrating that thrombin induces proliferation of microglia in primary culture (Suo et al., 2002). In addition, our previous study has shown that inhibition of p38 MAPK induces apoptotic cell death in striatal microglia and reduces the number of microglia in thrombin-treated slice cultures (Ohnishi et al., 2010). In the present study, we showed that an optimal concentration of ZnPP IX also induced apoptotic cell death in striatal microglia and reduced the number of microglia in thrombin-treated slice cultures. Therefore, these results indicate that HO-1 induction under control of p38 MAPK contributes to the maintenance of survival of activated microglia in the striatal region. Maintained survival of activated microglia should be harmful to neurons, as activated microglia produce diffusible cytotoxic factors such as nitric oxide and cytokines. Indeed, application of SB203580 or depletion of microglia almost completely inhibits thrombin-induced shrinkage of striatal tissue (Fujimoto et al., 2006). SB203580 also significantly attenuates the decrease in the number of striatal neurons after intracerebral hemorrhage *in vivo*, which was associated with a decrease in the number of activated microglia (Ohnishi et al., 2007).

Given the fact that ZnPP IX reduced the number of striatal microglia in thrombin-treated slice cultures, one would expect that this drug also attenuates thrombin-induced striatal injury. However, we observed only a marginal effect of ZnPP IX on thrombin-induced shrinkage of the striatal region. Moreover, the effect of ZnPP IX against thrombin-induced striatal shrinkage tended to disappear as the concentration of ZnPP IX increased. We have no definitive explanations for these results, although the effect of ZnPP IX on striatal shrinkage seems to closely correlate with that on the number of microglia. A fact to be considered is that ZnPP IX only partially decreased the number of activated microglia, which may not be sufficient to produce a significant protective effect on the viability of the striatal tissue.

Another possible cause is the involvement of HO-1 in cells other than microglia. That is, astrocytes in addition to the microglia expressed HO-1 in response to thrombin treatment, and HO-1 in astrocytes may be important for maintaining viability of these cells (Teng et al., 2004; Chen-Roetling et al., 2005). Since ZnPP IX does not discriminate HO-1 in different cell types, inhibition of HO-1 in astrocytes might reduce astrocyte-dependent tissue integrity and cancel the beneficial effect resulting from inhibition of HO-1 in microglia.

In contrast to the case with the striatal region, ZnPP IX showed a protective effect on cortical cell injury in a concentration-dependent manner. Totally distinct mechanisms are thought to mediate the protective effect of ZnPP IX in the cortical region than that in the striatal region because the mechanisms of thrombin-induced injury themselves differ between these two brain regions. A notable difference is that thrombin-induced cortical injury proceeds in a microglia-independent manner (Fujimoto et al., 2006). The fact that inhibition of p38 MAPK had no effect on cortical injury (Fujimoto et al., 2006) also highlights a different aspect of thrombin cytotoxicity in the cortex from that in the striatum. Therefore, HO-1-mediated acceleration of cortical injury should be explained irrespective of microglia as well as of p38 MAPK. Accordingly, we examined possible involvement of heme degradation products and found that supplementation of carbon monoxide by RuCO reversed the protective effect of ZnPP IX. These results present a novel mechanism of cytotoxicity in that generation of carbon monoxide may participate in thrombin-induced cortical cell injury. Finally, we should note that an iron chelator deferoxamine also provided a partial but significant protective effect against cortical injury. In this context, several reports have suggested involvement of iron in the pathogenesis of intracerebral hemorrhage (Hua et al., 2007; Wan et al., 2009).

Overall, the present study showed that HO-1 was involved in thrombin-induced pathology in the striatum and in the cortex, although the roles of HO-1 in these two brain regions were

different. In the striatum, HO-1 is induced in a p38 MAPK-dependent manner in activated microglia to inhibit microglial cell death. In the cortex, HO-1 accelerates cortical cell injury possibly via production of heme degradation products such as carbon monoxide. Manipulation of HO-1 expression, either in a brain region-specific manner or in a cell type-specific manner, may provide further insights into the roles of HO-1 in the pathogenesis of intracerebral hemorrhage and may lead to development of novel strategies to treat this devastating disorder.

EXPERIMENTAL PROCEDURES

Drugs and Chemicals

Drugs and chemicals were obtained from Nacalai Tesque (Kyoto, Japan), unless otherwise indicated. Thrombin from bovine plasma (catalog no. T4648), deferoxamine and tricarbonyldichlororuthenium (II) dimmer (RuCO) were obtained from Sigma-Aldrich (St. Louis, MO, USA). PD98059, SB203580 and zinc (II) protoporphyrin IX (ZnPP IX) were obtained from Calbiochem (San Diego, CA, USA). SP600125 was obtained from Tocris Cookson (Bristol, UK).

Preparation of Slice Cultures

Experimental procedures in the present study were approved by our institutional animal experimentation committee, and animals were treated in accordance with the Guidelines of the Unites States National Institutes of Health regarding the care and use of animals for experimental procedures. Organotypic slice cultures were prepared according to the methods described previously (Fujimoto et al., 2006; Ohnishi et al., 2009; Ohnishi et al., 2010). Briefly, Wistar rats at postnatal days 3–4 (Nihon SLC, Shizuoka, Japan) were anesthetized by hypothermia, and brains were removed from the skull and separated into two hemispheres. Each hemisphere was cut into coronal slices of 300 μm thickness under sterile conditions. Six corticostriatal tissue slices were transferred onto a 30-mm Millicell-CM insert membrane (Millipore, Bedford, MA, USA) in six-well plates. Culture medium, consisting of 50% minimum essential medium/HEPES (GIBCO, Invitrogen Japan, Tokyo, Japan), 25% Hanks' balanced salt solution (GIBCO), and 25% heat-inactivated horse serum (GIBCO) supplemented with 6.5 mg/ml D-glucose and 2 mM L-glutamine, 100 U/ml penicillin G potassium, and 100 μg/ml streptomycin sulfate (GIBCO), was supplied at 0.75 ml/well. Culture medium was exchanged for fresh one on the next day of culture

preparation, and thereafter, every 2 days. Slices were cultured in a humidified atmosphere of 5% CO_2 and 95% air at 34 °C.

Drug Treatment and Cell Death Assessment

Cultured slices at 9–11 days in vitro were incubated for 24–48 h in serum-free medium, where minimum essential medium/HEPES substituted for horse serum. Then slices were exposed to 100 U/ml thrombin and other drugs dissolved in serum-free medium for indicated periods. To assess cell injury, propidium iodide (5 μg/ml) was added to serum-free medium for thrombin treatment. Propidium iodide fluorescence was observed with an epifluorescence microscope equipped with a rhodamine filter set and a 10 × objective lens. Fluorescence images were captured through a monochrome chilled CCD camera (C5985; Hamamatsu Photonics, Hamamatsu, Japan). The intensity of each pixel was expressed as an 8-bit signal, and the average signal intensity in an area of 180 μm × 180 μm within the parietal cortex was obtained as the fluorescence value of each slice, with the use of NIH Image 1.63 software. Slice cultures treated with 100 μM *N*-methyl-D-aspartate for 72 h were used to determine the degree of the standard injury. Fluorescence values were normalized with the intensity in cultures that received standard injury as 100%. Images of whole slice cultures were also obtained through a 1 × objective lens. To estimate the area of the striatal region, we examined an image of propidium iodide fluorescence with increased gain, which revealed the entire morphology of a given slice probed by background fluorescence. With this image, we delineated the boundary of the striatal region and quantified the area with NIH Image 1.63 software.

Immunohistochemistry and Nuclear Staining

After drug treatment, slice cultures were fixed with 4% paraformaldehyde in 0.1 M

phosphate buffer containing 4% sucrose for 2 h. After rinsing with phosphate-buffered saline, they were permeabilized and blocked by 0.5% Triton X-100 in phosphate-buffered saline containing 3% goat or horse serum, then incubated with rabbit anti-MAP-2 (1:600; Sigma-Aldrich), rabbit anti-Iba1 (1:500; Wako Pure Chemicals, Osaka, Japan), rabbit anti-glial fibrillary acidic protein (GFAP; 1:1000; Dako A/S, Glostrup, Denmark), mouse anti-NeuN (1:200; Millipore), mouse anti-OX42 (1:300; Dainippon-Sumitomo Pharmaceutical, Osaka, Japan), mouse anti-GFAP (1:1000; Sigma-Aldrich), mouse anti-HO-1 (1:5000; Stressgen Bioreagents, Ann Arbor, MI, USA), and rabbit anti-phospho-p38 MAPK (T180/Y182) (1:50; Cell Signaling Technology) as primary antibodies overnight at 4 °C. After rinsing with phosphate-buffered saline, slices were incubated with Alexa Fluor 488-labeled goat anti-mouse IgG (1:200; Molecular Probes, Eugene, OR, USA), Alexa Fluor 594-labeled goat anti-rabbit IgG (1:200; Molecular Probes), and biotinylated anti-mouse IgG (1:200; Vector Laboratories, Burlingame, CA, USA) as secondary antibodies for 1 h at room temperature. After incubation with the biotinylated secondary antibody, slices were treated with avidin-biotinylated horseradish peroxidase complex (Vectastain Elite ABC kit, Vector Laboratories) and then peroxidase was visualized with diaminobenzine and H_2O_2. Bright-field images were captured through a monochrome chilled CCD camera and stored as image files. Immunofluorescence signals were acquired through a laser-scanning confocal microscopic system (MRC1024, BioRad, Hercules, CA, USA).

For observation of microglial nuclei, cultures processed for OX42 immunohistochemistry as mentioned above were incubated with 0.1 mg/ml Hoechst 33342 (Molecular Probes) for 15 min. Fluorescence signals were acquired through an epifluorescence microscope (BZ-8000, KEYENCE, Osaka, Japan).

Western blot analysis

After treatment with thrombin for the indicated periods, slices were harvested and homogenized in ice-cold lysis buffer containing 20 mM Tris–HCl (pH 7.0), 25 mM β-glycerophosphate (Sigma), 2 mM EGTA·2Na, 1% Triton X-100, 1 mM vanadate, 1% aprotinin (Sigma), 1 mM phenylmethylsulfonyl fluoride, and 2 mM dithiothreitol. Samples were mixed with a sample buffer composed of 124 mM Tris–HCl (pH 6.8), 4% sodium dodecyl sulfate (SDS), 10% glycerol, 0.02% bromophenol blue, and 4% 2-mercaptoethanol. After boiling for 5 min, samples were subjected to 12% SDS–polyacrylamide gel electrophoresis for around 90 min, followed by transfer to polyvinylidene difluoride membrane (Millipore) for 35 min. Membranes were blocked for at least 1 h by 5% nonfat milk at room temperature and subsequently incubated overnight with mouse anti-HO-1 (1:50,000) and anti-β-actin (1:100,000; Santa Cruz Biotechnology, Santa Cruz, CA, USA). The membranes were rinsed and incubated with ECL anti-rabbit IgG, horseradish peroxidase linked whole antibody (from donkey) (1:2000; GE Healthcare, UK). After incubating with secondary antibodies, membranes were rinsed, and bound antibodies were detected with Amersham ECL Western blotting detection reagents (GE Healthcare) according to the manufacturer's instructions.

Statistics

Data are expressed as means ± SEM. Statistical significance of difference was evaluated with one-way analysis of variance followed by Student–Newman–Keuls' test, unless otherwise indicated. When the data sets were not suitable for parametric tests, nonparametric Kruskal–Wallis test followed by Dunn's multiple comparisons test was used. Probability values less than 5% were considered significant.

ACKNOWLEDGMENTS

This work was supported by grants from The Smoking Research Foundation and Takeda Science Foundation, by a Grant-in-Aid for Scientific Research (20390026) from The Japan Society for the Promotion of Science, and by “Research for Promoting Technological Seeds A” program of Japan Science and Technology Agency.

LITERATURE REFERENCES

Alam, J., Stewart, D., Touchard, C., Boinapally, S., Choi, A.M., Cook, J.L., 1999. Nrf2, a Cap'n'Collar transcription factor, regulates induction of heme oxygenase-1 gene. J. Biol. Chem. 274:26071-26078.

Belayev, L., Saul, I., Busto, R., Danielyan, K., Vigdorchik, A., Khoutorova, L., Ginsberg, M.D., 2005. Albumin treatment reduces neurological deficit and protects blood-brain barrier integrity after acute intracortical hematoma in the rat. Stroke 36:326-331.

Chen, Y.C., Shen, S.C., Lee, W.R., Lin, H.Y., Ko, C.H., Lee, T.J., 2002. Nitric oxide and prostaglandin E_2 participate in lipopolysaccharide/interferon-gamma-induced heme oxygenase 1 and prevent RAW264.7 macrophages from UV-irradiation-induced cell death. J. Cell Biochem. 86:331-339.

Chen-Roetling, J., Benvenisti-Zarom, L., Regan, R.F., 2005. Cultured astrocytes from heme oxygenase-1 knockout mice are more vulnerable to heme-mediated oxidative injury. J. Neurosci. Res. 82:802-810.

Doré, S., Takahashi, M., Ferris, C.D., Zakhary, R., Hester, L.D., Guastella, D., Snyder, S.H., 1999. Bilirubin, formed by activation of heme oxygenase-2, protects neurons against oxidative stress injury. Proc. Natl. Acad. Sci. USA. 96:2445-2450.

Flynn, A.N., Buret, A.G., 2004. Proteinase-activated receptor 1 (PAR-1) and cell apoptosis. Apoptosis 9:729-737.

Fujimoto, S., Katsuki, H., Kume, T., Akaike, A., 2006. Thrombin-induced delayed injury involves multiple and distinct signaling pathways in the cerebral cortex and the striatum in organotypic slice cultures. Neurobiol Dis 22:130-142.

Fujimoto, S., Katsuki, H., Ohnishi, M., Takagi, M., Kume, T., Akaike, A., 2007. Thrombin induces striatal neurotoxicity depending on mitogen-activated protein kinase pathways in vivo. Neuroscience 144:694-701.

Hua, Y., Keep, R.F., Hoff, J.T., Xi, G., 2007. Brain injury after intracerebral hemorrhage: The role of thrombin and iron. Stroke 38:759-762.

Huang, Y.N., Wu, C.H., Lin, T.C., Wang, J.Y., 2009. Methamphetamine induces heme oxygenase-1 expression in cortical neurons and glia to prevent its toxicity. Toxicol. Appl. Pharmacol. 240:315-326.

Hwang, Y.P., Jeong, H.G., 2008. The coffee diterpene kahweol induces heme oxygenase-1 via PI3K and p38/Nrf2 pathway to protect human dopaminergic neurons from 6-hydroxydopamine-derived oxidative stress. FEBS Lett. 582:2655-2662.

Kitaoka, T., Hua, Y., Xi, G., Hoff, J.T., Keep, R.F., 2002. Delayed argatroban treatment reduces edema in a rat model of intracerebral hemorrhage. Stroke 33:3012-3018.

Lee, T.S., Tsai, H.L., Chau, L.Y., 2003. Induction of heme oxygenase-1 expression in murine macrophages is essential for the anti-inflammatory effect of low dose 15-deoxy-delta 12,14-prostaglandin J_2. J. Biol. Chem. 278:19325-19330.

Maines, M.D., 1988. Heme oxygenase: function, multiplicity, regulatory mechanisms, and clinical applications FASEB J. 2:2557-2568.

Marinissen, M.J., Servitja, J.M., Offermanns, S., Simon, M.I., Gutkind, J.S., 2003. Thrombin protease-activated receptor-1 signals though Gq- and G13-initiated MAPK cascades regulating c-Jun expression to induce cell transformation. J. Biol. Chem. 278:46814-46825.

Noobakhsh, F., Vergnolle, N., Hollenberg, M.D., 2003. Proteinase-activated receptors in the nervous system. Nat Rev Neurosci 4:981-990.

Ohnishi, M., Katsuki, H., Fujimoto, S., Takagi, M., Kume, T., Akaike, A., 2007. Involvement of thrombin and mitogen-activated protein kinase pathways in hemorrhagic brain injury. Exp Neurol 206:43-52.

Ohnishi, M., Katsuki, H., Takagi, M., Kume, T., Akaike, A., 2009. Long-term treatment with

nicotine suppresses neurotoxicity of, and microglial activation by, thrombin in cortico-striatal slice cultures. Eur J Pharmacol 602:288-293.

Ohnishi, M., Katsuki, H., Izumi, Y., Kume, T., Takada-Takatori, Y., Akaike, A., 2010. Mitogen-activated protein kinases support survival of activated microlgia that mediate thrombin-induced striatal injury in organotypic slice culture. J. Neurosci. Res. 88:2155-2164.

Park, H.K., Chu, K., Lee, S.T., Jung, K.H., Kim, E.H., Lee, K.B., Song, Y.M., Jeong, S.W., Kim, M., Roh, J.K., 2005. Granulocyte colony-stimulating factor induces sensorimotor recovery in intracerebral hemorrhage. Brain Res. 1041:125-131.

Prestera, T., Talalay, P., Alam, J., Ahn, Y.L., Lee, P.J., Choi, A.M., 1995. Parallel induction of hemeoxygenase-1 and chemoprotective phase 2 enzymes by electrophiles and antioxidants: regulation by upstream antioxidant-responsive element (ARE). Mol. Med. 1:827-37.

Ryter, S.W., Alam, J., Choi, A.M., 2006. Heme oxygenase-1/carbon monoxide: from basic science to therapeutic applications. Physiol. Rev. 86:583-650.

Lee, S., Suk, K., 2007. Heme oxygenase-1 mediates cytoprotective effects of immunostimulation in microglia. Biochem. Pharmacol. 74:723-729.

Striggow, F., Riek-Burchardt, M., Kiesel, A., Schmidt, W., Henrich-Noack, P., Breder, J., Krug, M., Reymann, K.G., Reiser, G., 2001. Four different types of protease-activated receptors are widely expressed in the brain and are up-regulated in hippocampus by severe ischemia. Eur. J. Neurosci. 14:595-608.

Suo, Z., Wu, M., Ameenuddin, S., Anderson, H.E., Zoloty, J.E., Citron, B.A., Andrade-Gordon, P., Festoff, B.W., 2002. Participation of protease-activated receptor-1 in thrombin-induced microglial activation. J. Neurochem. 80:655-666.

Suo, Z., Wu, M., Citron, BA., Palazzo, R.E., Festoff, BW., 2003. Rapid tau aggregation and

delayed hippocampal neuronal death induced by persistent thrombin signaling. J. Biol. Chem. 278:37681-37689.

Teng, Z.P., Chen, J., Chau, L.Y., Galunic, N., Regan, R.F., 2004. Adenoviral transfer of the heme oxygenase-1 gene protects cortical astrocytes from heme-mediated oxidative injury. Neurobiol. Dis. 17:179-187.

Xi, G., Keep, R.F., Hoff, J.T., 2006. Mechanisms of brain injury after intracerebral hemorrhage. Lancet Neurol. 5:53-63.

Yamamoto, N., Izumi, Y., Matsuo, T., Wakita, S., Kume, T., Takada-Takatori, Y., Sawada, H., Akaike, A., 2010. Elevation of heme oxygenase-1 by proteasome inhibition affords dopaminergic neuroprotection. J. Neurosci. Res. 88:1934-1942.

Wan, S., Zhan, R., Zheng, S., Hua, Y., Xi, G., 2009. Activation of c-Jun-N-terminal kinase in a rat model of intracerebral hemorrhage: the role of iron. Neurosci. Res. 63:100-105.

Wang, H., Ubl, J.J., Stricker, R., Reiser, G., 2002. Thrombin (PAR-1)-induced proliferation in astrocytes via MAPK involves multiple signaling pathways Am. J. Physiol. Cell Physiol. 283:C1351-C1364.

Wang. J., Doré. S., 2007. Heme oxygenase-1 exacerbates early brain injury after intracerebral hemorrhage. Brain 130:1643-1652.

Figure legends

Fig. 1. Effect of ZnPP IX, a HO-1 inhibitor, on thrombin-induced injury. (**A**–**F**) Representative images of propidium iodide fluorescence of whole slice cultures after 72 h of treatment with 100 U/ml thrombin in the absence and the presence of 0.3–3 μM ZnPP IX. Broken lines indicate areas of the cerebral cortex (Cx) and the striatum (St). Scale bar = 1 mm. (**G**) Summary of the effect of ZnPP IX on thrombin-induced cortical cell injury as assessed by the intensity of propidium iodide fluorescence. (**H**) Summary of the effect of ZnPP IX on thrombin-induced shrinkage of the striatal tissue. The number of slices examined for each condition ranged between 36 and 48. *** $P < 0.001$ vs. control; $^{\#\#}$ $P < 0.01$, $^{\#\#\#}$ $P < 0.001$ vs. thrombin alone.

Fig. 2. Thrombin-induced HO-1 expression. (**A**) Representative blots of HO-1 expression in response to thrombin. Homogenates were prepared from whole slice cultures treated with 100 U/ml thrombin for indicated periods, and lysates were subjected to Western blot analysis with specific antibodies against HO-1 and β-actin. Slices without thrombin treatment (0 h) were used as control. (**B**) Time course of HO-1 expression. Ratio of HO-1 vs. β-actin at each time point was normalized by the ratio at time 0. n = 4. (**C**–**K**): Confocal microscopic images of immunofluorescence of HO-1 with MAP-2 (C–E), Iba1 (F–H), or GFAP (I–K) and their merged images (E, H, K) in slice cultures treated with thrombin for 24 h. Arrows indicate colocalization. Scale bar = 50 μm.

Fig. 3. Effects of MAP kinase inhibitors on thrombin-induced HO-1 expression. (**A**) Western blot analysis was performed on slice cultures that received 100 U/ml thrombin treatment with or without PD98059 (PD; 100 μM), SB203580 (SB; 100 μM), and SP600125 (SP; 100 μM) for 24 h. (**B**) Summary of the effects of MAP kinase inhibitors on HO-1

expression. $^{\#}P < 0.05$ vs. thrombin alone, based on nonparametrical Kruskal–Wallis test followed by Dunn's multiple comparisons test (n = 4).

Fig. 4. Identification of cell types that exhibit p38 MAPK activation in response to thrombin treatment. Shown are confocal microscopic images of immunofluorescence of phosphorylated p38 MAPK (P-p38; B, E, H) with NeuN (A), OX42 (D), or GFAP (G) and their merged images (C, F, I) in slice cultures treated with 100 U/ml thrombin for 1 h. Arrows indicate colocalization. Scale bar = 50 μm.

Fig. 5. Microglial apoptosis induced by HO-1 inhibitor. (**A-C)** Representative images of OX42-immunostained slices after 72 h of treatment with 100 U/ml thrombin. Where indicated, 0.3 μM ZnPP IX was concomitantly applied for 72 h. Scale bar = 100 μm. (**D)** Summary of the effect of ZnPP IX (0.3–3 μM) on thrombin-induced increase in the number of OX42-positive cells in the striatal region. The number of slices examined for each condition ranged between 12 and 18. *** $P < 0.001$ vs. control; $^{\#\#}P < 0.01$ vs. thrombin alone. (**E–H)** Hoechst 33342 nuclear staining of striatal microglia after 48 h of treatment with 100 U/ml thrombin in the absence and the presence of 0.3 μM ZnPP IX. Arrows indicate condensed nuclei of OX42-positive microglia. Panel H is a magnified view of the area denoted by a square in panel G. Scale bar = 50 μm (E–G) and 5 μm (H). (**I)** Summary of the effect of ZnPP IX combined with thrombin on the appearance of apoptotic nuclei in striatal microglia. The number of slices examined for each condition ranged between 9 and 12. $^{\#\#\#}P < 0.001$ vs. thrombin alone.

Fig. 6. Contribution of heme catabolites to thrombin-induced injury of cortical cells. (**A)** Effect of RuCO (10–100 μM) on the protective effect of 3 μM ZnPP IX against thrombin

(100 U/ml)-induced cortical cell injury. Drugs were concomitantly applied for 72 h, and cortical cell injury was assessed by the intensity of PI fluorescence. The number of slices examined for each condition ranged between 18 and 24. *** $P < 0.001$ vs. control; $^{###}$ $P < 0.001$ vs. thrombin alone; $^{+}$ $P < 0.05$, $^{+++}$ $P < 0.001$ vs. thrombin plus ZnPP IX. **(B)** Effect of concomitant application of deferoxamine (3–30 μM) on cortical cell injury induced by 72 h of treatment with 100 U/ml thrombin. The number of slices examined for each condition ranged between 24 and 42. *** $P < 0.001$ vs. control; $^{\#}$ $P < 0.05$ vs. thrombin alone.

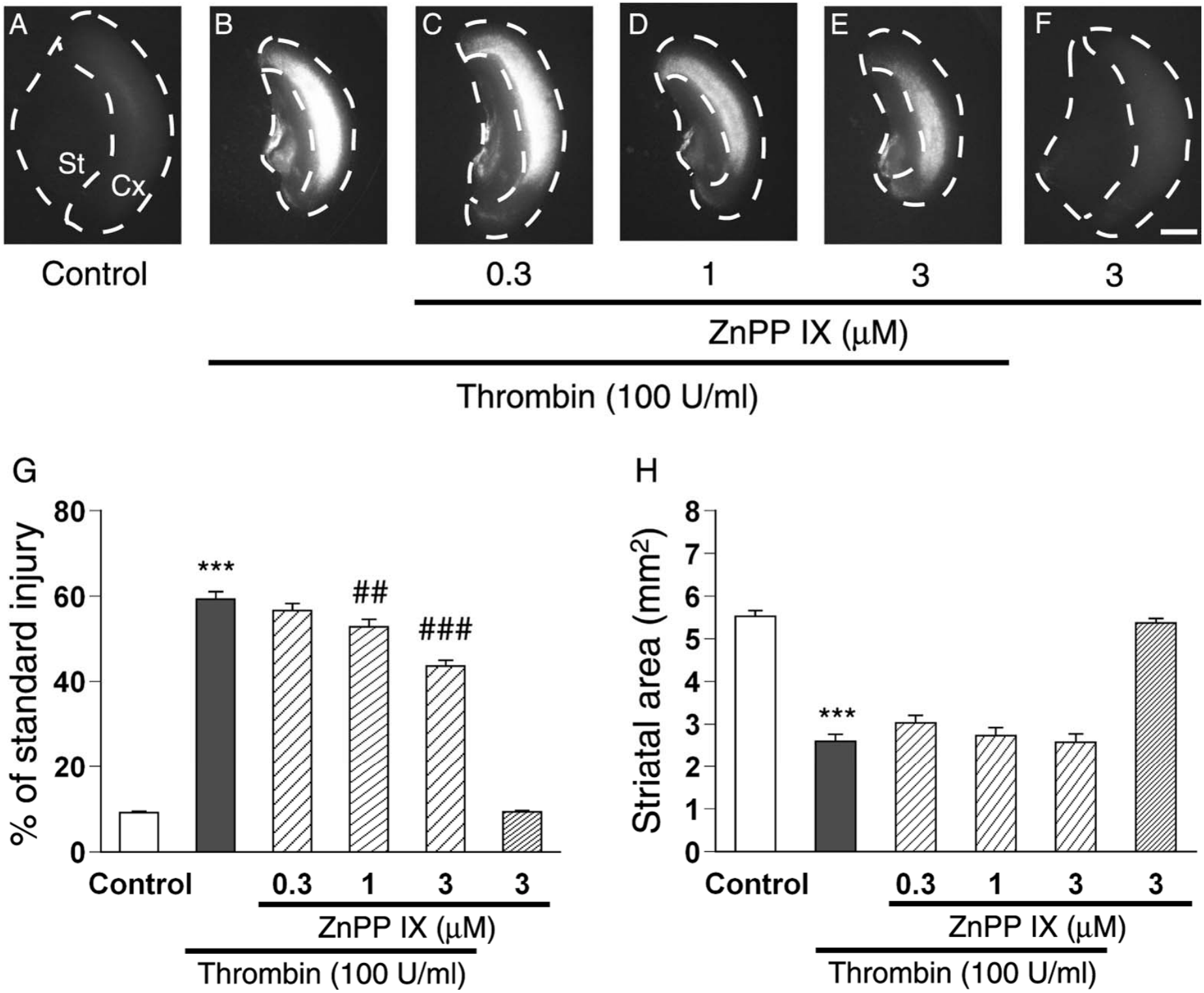
A
B
C
D
E
F
St
Cx
Control
0.3
1
3
3
ZnPP IX (μM)
Thrombin (100 U/ml)
G
% of standard injury
80
60
40
20
0
***
##
###
Control
0.3
1
3
3
ZnPP IX (μM)
Thrombin (100 U/ml)
H
Striatal area (mm2)
8
7
6
5
4
3
2
1
0
***
Control
0.3
1
3
3
ZnPP IX (μM)
Thrombin (100 U/ml)

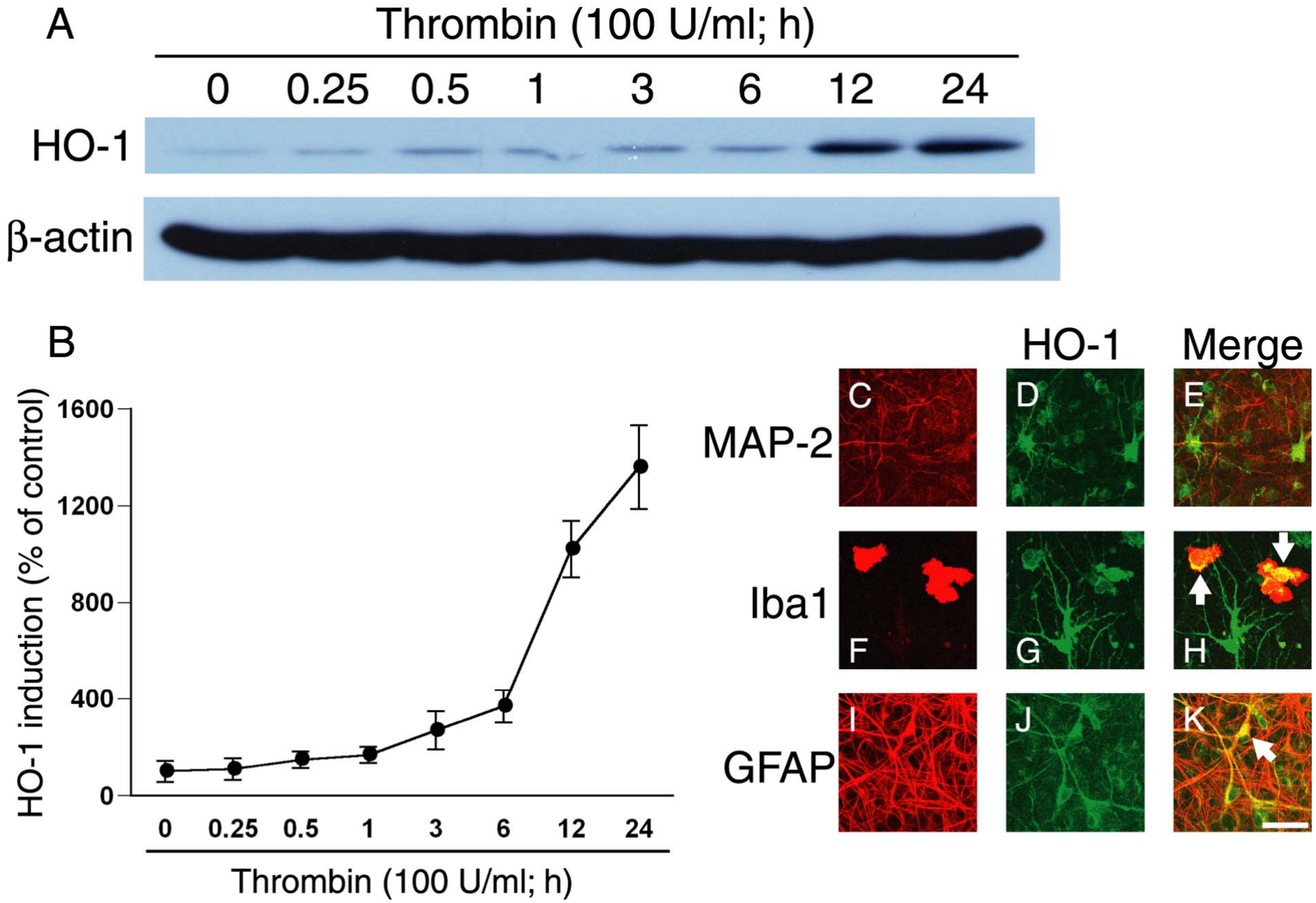
A
Thrombin (100 U/ml; h)
0
0.25
0.5
1
3
6
12
24
HO-1
β-actin
B
HO-1 induction (% of control)
1600
1200
800
400
0
0
0.25
0.5
1
3
6
12
24
Thrombin (100 U/ml; h)
HO-1
Merge
MAP-2
Iba1
GFAP
C
D
E
F
G
H
I
J
K

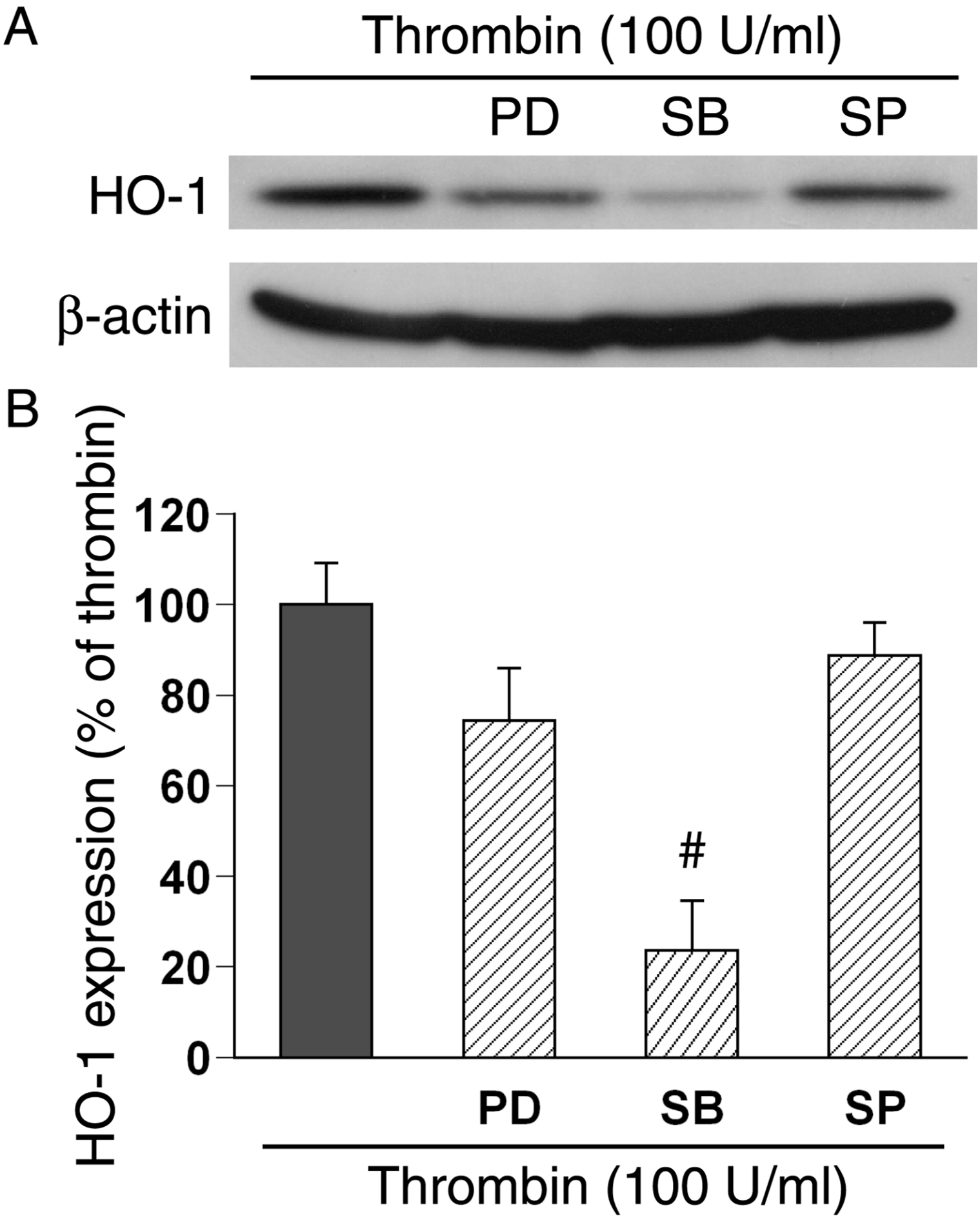
A
Thrombin (100 U/ml)
PD
SB
SP
HO-1
β-actin
B
HO-1 expression (% of thrombin)
120
100
80
60
40
20
0
#
PD
SB
SP
Thrombin (100 U/ml)

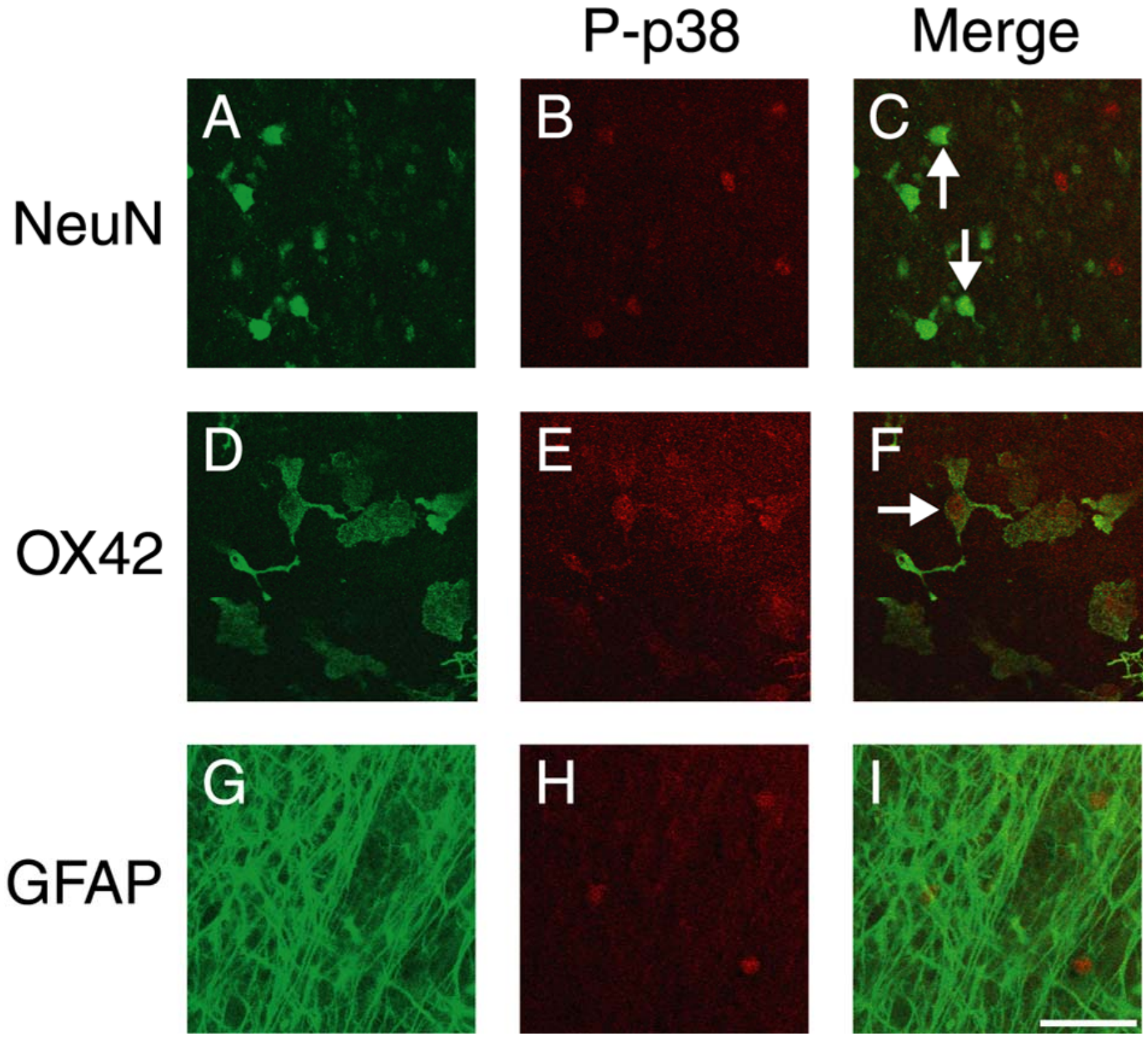
P-p38
Merge
NeuN
OX42
GFAP
A
B
C
D
E
F
G
H
I

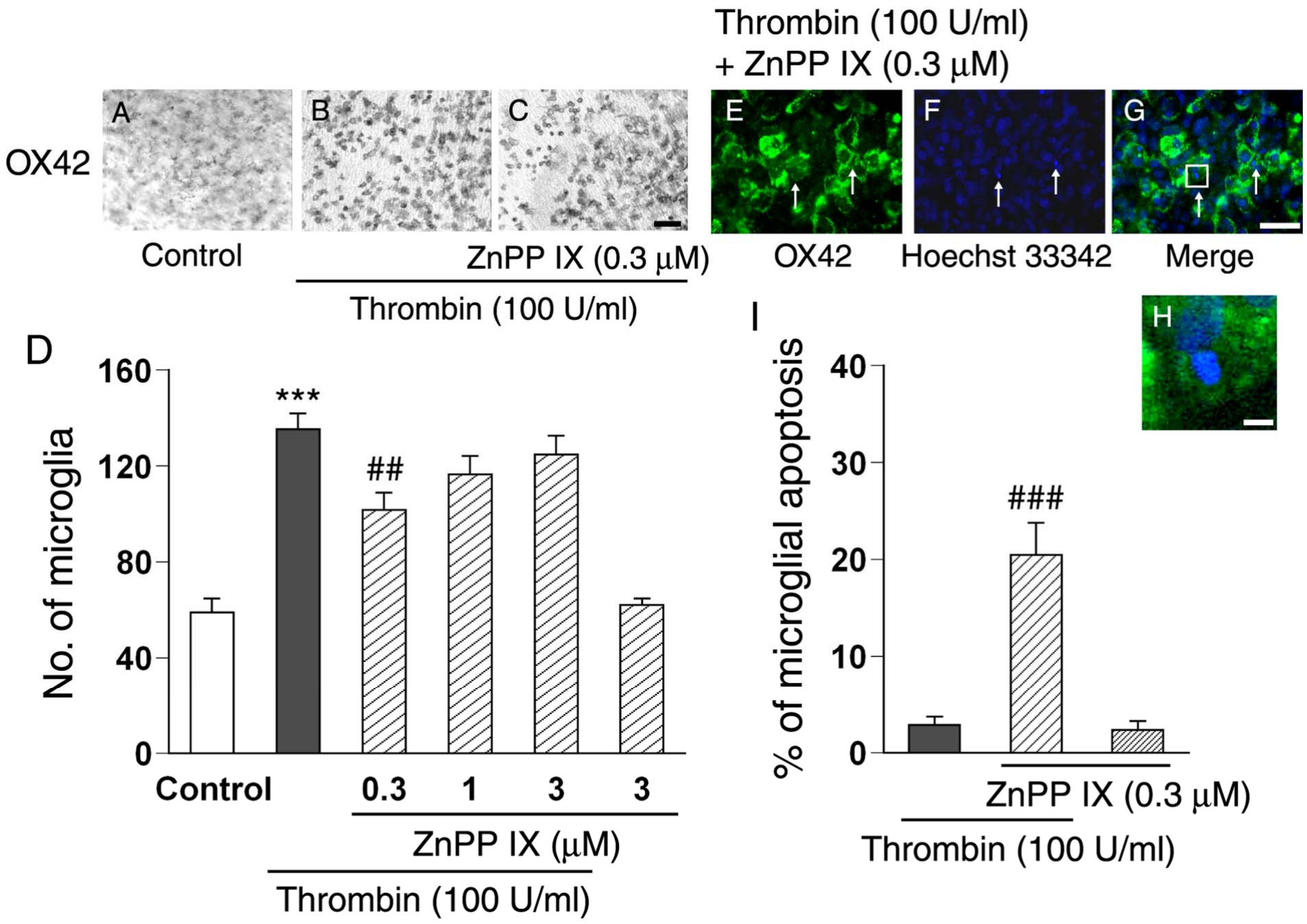
Thrombin (100 U/ml)
+ ZnPP IX (0.3 μM)
OX42
A
B
C
E
F
G
Control
ZnPP IX (0.3 μM)
Thrombin (100 U/ml)
OX42
Hoechst 33342
Merge
D
No. of microglia
160
120
80
40
0
***
##
Control
0.3
1
3
3
ZnPP IX (μM)
Thrombin (100 U/ml)
I
H
% of microglial apoptosis
40
30
20
10
0
###
ZnPP IX (0.3 μM)
Thrombin (100 U/ml)

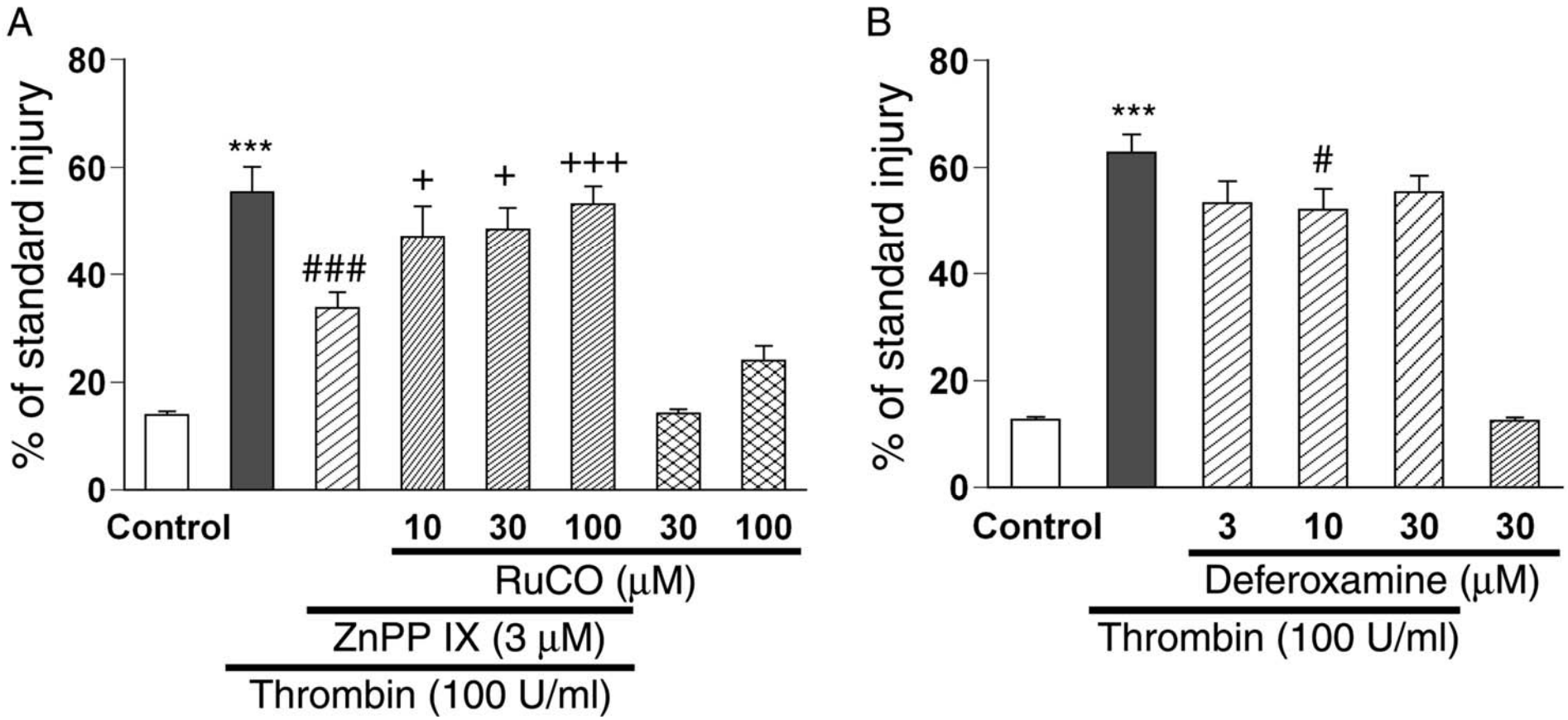
A
% of standard injury
80
60
40
20
0
***
###
+
+
+++
Control
10
30
100
30
100
RuCO (μM)
ZnPP IX (3 μM)
Thrombin (100 U/ml)
B
% of standard injury
80
60
40
20
0
***
#
Control
3
10
30
30
Deferoxamine (μM)
Thrombin (100 U/ml)